Title

Mutations in the gene encoding 3β- hydroxysteroid-Δ8,Δ7- isomerase cause X-linked dominant Conradi-Hünermann syndrome

Journal

Nature Genetics, 22(3)

ISSN

1061-4036

Authors

Braverman, Nancy
Lin, Paul
Moebius, Fabian F
et al.

Publication Date

1999-07-01

DOI

10.1038/10357

Mutations in the gene encoding 3β-hydroxysteroid-Δ^8,Δ^7-isomerase cause X-linked dominant Conradi-Hünermann syndrome

Nancy Braverman[1], Paul Lin[2], Fabian F. Moebius[3], Cassandra Obie[2], Ann Moser[4], Hartmut Glossmann[5], William R. Wilcox[6], David L. Rimoin[6], Moyra Smith[7], Lisa Kratz[1,4], Richard I. Kelley[1,4] & David Valle[1,2]

X-linked dominant Conradi-Hünermann syndrome (CDPX2; MIM 302960) is one of a group of disorders with aberrant punctate calcification in cartilage, or chondrodysplasia punctata (CDP). This is most prominent around the vertebral column, pelvis and long bones in CPDX2. Additionally, CDPX2 patients may have asymmetric rhizomesomelia, sectorial cataracts, patchy alopecia, ichthyosis and atrophoderma[1]. The phenotype in CDPX2 females ranges from stillborn to mildly affected individuals identified in adulthood. CDPX2 is presumed lethal in males, although a few affected males have been reported[2,3]. We found increased 8(9)-cholestenol and 8-dehydrocholesterol in tissue samples from seven female probands with CDPX2 (ref. 4). This pattern of accumulated cholesterol intermediates suggested a deficiency of 3β-hydroxysteroid-Δ^8,Δ^7-isomerase (sterol-Δ^8-isomerase), which catalyses an intermediate step in the conversion of lanosterol to cholesterol[4]. A candidate gene encoding a sterol-Δ^8-isomerase (*EBP*) has been identified and mapped to Xp11.22–p11.23 (refs 5,6). Using SSCP analysis and sequencing of genomic DNA, we found *EBP* mutations in all probands. We confirmed the functional significance of two missense alleles by expressing them in a sterol-Δ^8-isomerase-deficient yeast strain. Our results indicate that defects in sterol-Δ^8-isomerase cause CDPX2 and suggest a role for sterols in bone development.

Because of the occasional occurrence of CDP in Smith-Lemli-Opitz (SLO) syndrome (MIM 270400), which is caused by 7-dehydrocholesterol reductase deficiency[7,8], we sought to determine if another defect in cholesterol biosynthesis might be responsible for the CDPX2 phenotype. We obtained tissue samples from seven unrelated female probands with CDP (Table 1). Three had a clinical diagnosis of CDPX2. The remainder were unclassified, but had both skeletal and clinical features consistent with CDPX2. Clinical and biochemical data on patients 1–5 have been reported[4]. All samples showed accumulation of 8(9)-cholestenol and 8-dehydrocholesterol by gas chromatography/mass spectroscopy (GC/MS). This pattern of accumulated sterol intermediates suggested a defect at C8-C7 isomerization, a reaction catalysed by sterol-Δ^8-isomerase (Fig. 1*a*, step 1). The GC profile of fibroblast sterols from patient 6, grown in a cholesterol-free medium, and sterol levels from patients 6 (fibroblasts) and 7 (liver, twin A and B) are shown (Fig. 1*b*). The elevation of lathosterol and normal levels of 7-dehydrocholesterol, cholesterol and desmosterol (latter not shown) presumably reflect upregulation of cholesterol biosynthesis in neighbouring cells with normal sterol-Δ^8-isomerase activity[9].

On the basis of these clinical and biochemical abnormalities, we considered *EBP* (refs 5,6), located at Xp11.22–p11.23, a candidate for CDPX2. *EBP* spans 7.0 kb of genomic DNA and comprises 5 exons encoding a 1.0-kb mature transcript with ubiquitous expression. The intron-exon splice sites and their locations in the cDNA are shown (Table 2). The ORF encodes a protein (of 230 aa) predicted to be an integral endoplasmic reticulum (ER) membrane protein with four transmembrane domains. Sterol-Δ^8-isomerase was originally isolated in guinea pig as a phenylalkylamine Ca^{2+} antagonist (emopamil) binding protein and shown to form homodimers in the ER (ref. 10). Isolation of the mouse orthologue by functional complementation of yeast deficient in sterol-Δ^8-isomerase activity determined that the emopamil binding protein was a sterol-Δ^8-isomerase[11]. The human sterol-Δ^8-isomerase shows 78%, 73% and 37% amino acid identity with its mouse, guinea pig and *Arabidopsis thaliana* orthologues, respectively[12].

To determine if defects in sterol-Δ^8-isomerase are responsible for CDPX2, we screened PCR-amplified genomic DNA fragments for each exon, including intron junctions, by SSCP from the seven

Table 1 • Clinical and molecular data

Patient	Diagnosis	Family history[a]	Age at diagnosis	Ethnicity	Diagnostic tissues	Nucleotide change	Exon	Mutant protein	Predicted consequence
2	CDPX2	+	7 yr	European	connective tissue	238G→A	2	E80K	missense
6	CDPX2	+	13 yr	Hispanic	fibroblasts	187C→T	2	R63X	nonsense
5	CDPX2	+	25 wk[b]	unknown	cartilage, fibroblasts	216–217insT	2	C72fs	frameshift
4	CDP	+	30 wk[c]	unknown	connective tissue	IVS3+1G→T	3		abnormal splicing
7A	CDP	–	31 wk[c]	European	liver, fibroblasts	IVS2–2delA	3		abnormal splicing
1	CDP	–	birth[d]	Polynesian	plasma, lymphoblasts	399C→G	4	S133R	missense
3	CDP	+	21 wk[b]	unknown	connective tissue, fibroblasts	440G→A	4	R147H	missense

[a]First-degree female relative with skeletal and skin abnormalities consistent with CDPX2. [b]Elective termination of pregnancy. [c]Spontaneous miscarriage. [d]Term death.

[1]Department of Pediatrics, [2]Howard Hughes Medical Institute, [3]Department of Biological Chemistry and [4]Kennedy Krieger Institute, Johns Hopkins University School of Medicine, Baltimore, Maryland 21205, USA. [5]Institut für Biochemische Pharmakologie, Innsbruck, Austria. [6]Burns and Allen Cedars Sinai Research Institute, Department of Pediatrics, UCLA School of Medicine, Los Angeles, California 90048, USA. [7]Department of Pediatrics, University of California, Irvine, California 92697, USA. Correspondence should be addressed to D.V. (e-mail: dvalle@jhmi.edu).

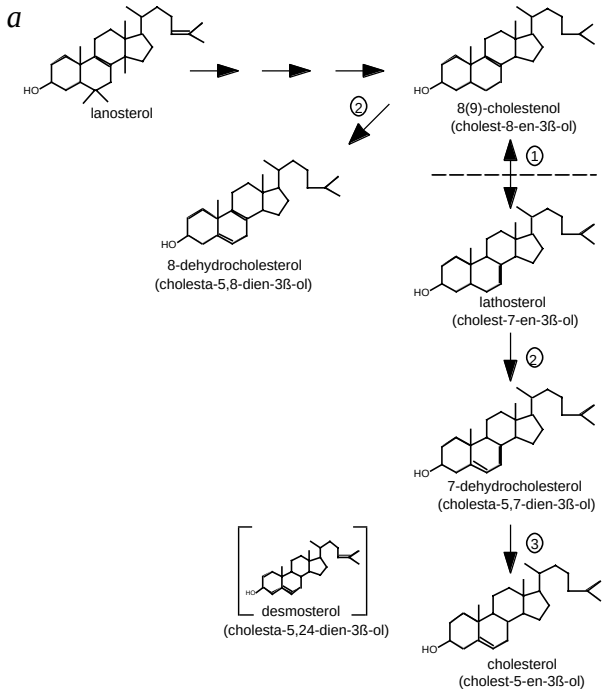

Samples	8-Dehydro-cholesterol	8(9)-cholestenol	Lathosterol	7-Dehydro-cholesterol	Cholesterol
Fibroblasts[a]					
patient 6	0.51	7.00	0.41	0.05	16.9
normal mean	0.02	0.05	0.05	0.02	21.1
s.d.(n=5)	0.02	0.10	0.03	0.03	2.9
Liver[b]					
twin 7A	0.64	5.08	1.52	0.01	92.5
twin 7B	0.44	3.18	0.66	0.01	95.9
non-CDP liver	<0.01	<0.01	0.50	0.03	98.3

[a]µg/mg protein, [b]Per cent of total sterols.

Fig. 1 Sterol metabolism in CPDX2. ***a***, Schematic of the principal 27-carbon sterol intermediates derived from 30-carbon lanosterol and comprising the distal Kandutsch-Russell pathway for cholesterol biosynthesis. The denoted enzymatic steps are: (1), 3β-hydroxysteroid-Δ^8,Δ^7-isomerase (EC 5.3.3.5), defective in CDPX2; (2), 3β–hydroxysteroid-Δ^5-desaturase (lathosterol dehydrogenase; EC 1.3.3.2); and (3), 3β–hydroxysteroid-Δ^7-reductase (7-dehydrocholesterol reductase, EC 1.3.1.21), defective in SLO syndrome. The C24-C25 double bond can be reduced by 3β–hydroxysteroid-Δ^{24}-reductase at several steps along the pathway. Deficiency of this enzyme results in the accumulation of desmosterol, shown in brackets. ***b***, Sterol patterns in CDPX2. Top, GC flame ionization profile of normal (left) and patient 6 (right) fibroblast sterols. The abscissa is elution time and the ordinate, detector response in arbitrary units. The major identified compounds are: (1) internal standard (epicoprostanol); (2) cholesterol; (3) 8–dehydrocholesterol; (4) 8(9)-cholestenol; (5) desmosterol; (6) lathosterol. Note that peaks 3 and 4 are barely detectable in normal fibroblasts. Bottom, quantified sterols in tissues from patients 6, 7A and 7B.

probands. We found heterozygous mutations in each proband including three missense (E80K, S133R, R147H), one nonsense (R63X), one frameshift (216–217insT) and two splice-site (IVS2-2delA, IVS3+1G→T; Fig. 2 and Table 1) mutations. Additionally, we found a G→T transversion at bp 15 that is a synonymous mutation (A5A) present in 16 of 40 isomerase genes studied. The nonsense, frameshift and splice-site mutations delete more than one-third of the protein and are highly likely to be functionally significant. All three missense alleles involve substitutions of conserved amino acids. E80 and S133 are located in transmembrane domains and are conserved among mammalian and plant sterol-Δ^8-isomerases. R147 is predicted to be in a loop inside the ER and is conserved in mammals only. E80 is required for both catalytic activity and inhibitor binding of sterol-Δ^8-isomerase[12].

To test directly the functional significance of the missense alleles, we expressed them in a *Saccharomyces cerevisiae* strain deficient in sterol-Δ^8-isomerase[13] (*erg2-3*). The *erg2-3* mutant accumulates Δ^8-sterols and this biochemical phenotype is corrected by expression of wild-type human sterol-Δ^8-isomerase[11,12]. We produced E80K, S133R and R147H sterol-Δ^8-isomerase alleles by PCR mutagenesis, subcloned them into a 2 µ-based yeast expression vector and introduced them into *erg2-3* yeast. We used GC/MS to analyse sterols extracted from the transformed yeast. Transformed mutant yeast expressing wild-type human isomerase showed reduced Δ^8- and $\Delta^{5,8}$-sterols and accumulation of the $\Delta^{5,7}$-sterol ergosterol, the primary structural sterol in yeast (Fig. 3*a*,*b*). This pattern is similar to that in wild-type yeast (data not shown). In cells expressing the E80K and S133R alleles, we observed no correction of sterol metabolites and ergosterol levels were similar to those in mutant cells transformed with vector alone (Fig. 3*a*,*c*). In support of these expression data, we also surveyed 170 control isomerase genes for E80K and 212 for S133R and found none (data not shown). We conclude that these two missense alleles are functionally inactive and are not polymorphic. Expression of the R147H allele in yeast increased ergosterol levels, but not to the same extent as wild type (Fig. 3*b*,*d*). An N-myc–tagged version of each missense allele was expressed in a similar fashion and shown to be present on immunoblots (Fig. 4), verifying that both wild-type and mutant human proteins are stable in this heterologous system. Because R147H showed some Δ^8-isomerase activity, we considered that it may be a normal variant present at polymorphic frequencies in the general population. In a survey of 212 control isomerase genes by allele-specific oligonucleotide (ASO) analysis, however, we found no R147H alleles (data not shown). We favour the inter-

Table 2 • Intron-exon boundaries of *EBP*[a]

Exon	Exon size (bp)	5′ bp[b]	3′ splice site	Exon	5′ splice site	Intron size (kb)
1	39	–111			.....CCTTGgtgagtgccc	1.6
2	375	–73	atttgtccagGTTTT	.....	ACTCTgtgagtcctc	2.9
3	37	302	ttttcttcagGGAAA	.....	ATCCTgtaatggttt	0.2
4	131	339	tctcctgcagGGTGG	.....	TGTGGgtaaggaaag	0.9
5	483[c]	425	ccacccacagGCCAG	.....		

[a]Sequenced by the Institut für Molekulare Biotechnologie, Genome Sequencing Centre, Jena. [b]The adenine of the initiation codon ATG is designated +1. [c]Length of the last nucleotide before the 3′ poly(A) tract.

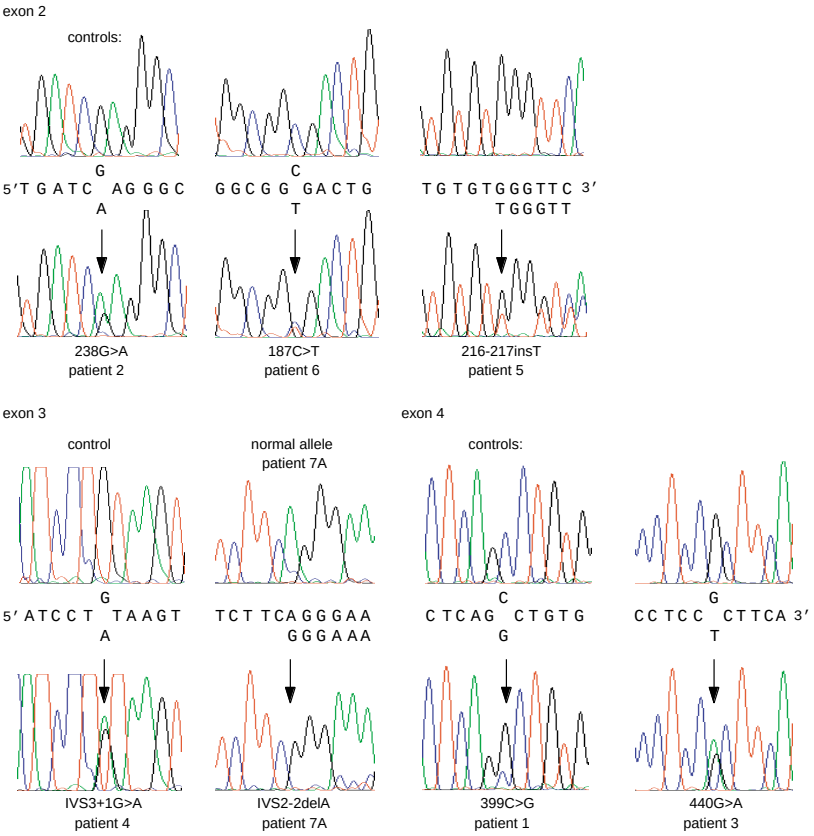

Fig. 2 Heterozygous mutations in *EBP* in all seven probands. Sequences are arranged by exon. Normal sequence is shown above each patient sequence. Genomic DNA fragments were amplified and sequenced directly, except for patient 7A, in which the amplified genomic DNA fragment containing exon 3 was cloned and then sequenced.

pretation that R147H is a functionally significant mutation, but because of high expression from the multicopy vector, the activity is sufficient to partially correct the biochemical phenotype of the mutant yeast.

We found no obvious correlation between the molecular defects in the seven probands and the severity of their clinical phenotypes. Lyonization is an important variable determining the phenotypic severity of X-linked disorders and may obscure any direct relationship between genotype and phenotype. We presume that *EBP* is subject to X inactivation because it is located in a region of the X (Xp11.22–p11.23) where many of the genes undergo inactivation[6] and because of the mosaic nature of the phenotypic features of CDPX2 (for example the skin and bone involvement). Direct studies of X-inactivation patterns in CDPX2 will be necessary to confirm this. Additionally, our results do not rule out the possibility that the aetiology of the CDPX2 phenotype is heterogeneous. Although it was thought that the X-linked dominant bare patches mouse (*Bpa*) would be a model for CDPX2 (ref. 14), a defect in the gene encoding 3β-hydroxysteroid dehydrogenase (which maps to Xq28 in human) has recently been reported in *Bpa* (ref. 15). Thus, some patients with the CDPX2 phenotype may have defects in a 3β-hydroxysteroid dehydrogenase involved in sterol synthesis.

We have shown here that defects in sterol-Δ^8-isomerase cause CDPX2. This is the second documented human disorder of the post-squalene cholesterol biosynthetic pathway. The first, 3β-hydroxysteroid-Δ^7-reductase deficiency[7,8] (Fig. 1*a*, step 3), causes SLO, a multiple congenital anomaly syndrome with rhizomelia, cataracts and occasionally CDP. Additionally, accumulation of desmosterol, suggesting 3β-hydroxysteroid-Δ^{24}-reductase deficiency (Fig. 1*a*), was recently described in a stillborn infant with rhizomesomelia, skeletal dysplasia, cataracts and other birth defects[16]. The overlapping developmental phenotypes of these three disorders suggest that relative cholesterol deficiency, or the accumulation of a teratogenic sterol precursor, may be a common pathogenic factor in skeletal abnormalities[17]. Cholesterol and related metabolites are important components of cell membranes and are required for proper functioning of hedgehog (HH) signalling pathways[18]. It is interesting to speculate that cell autonomous sterol abnormalities in CDPX2 might impair the function of Indian HH (IHH), a HH protein required for vertebrate skeletal development. Mice with induced mutations in this pathway[19–21] show accelerated chondrocyte differentiation resulting in abnormal growth plates and ectopic calcification[21]. In CDPX2 there is loss of chondrocytes in reserve cartilage and degeneration of the cartilage matrix; the growth plate is abnor-

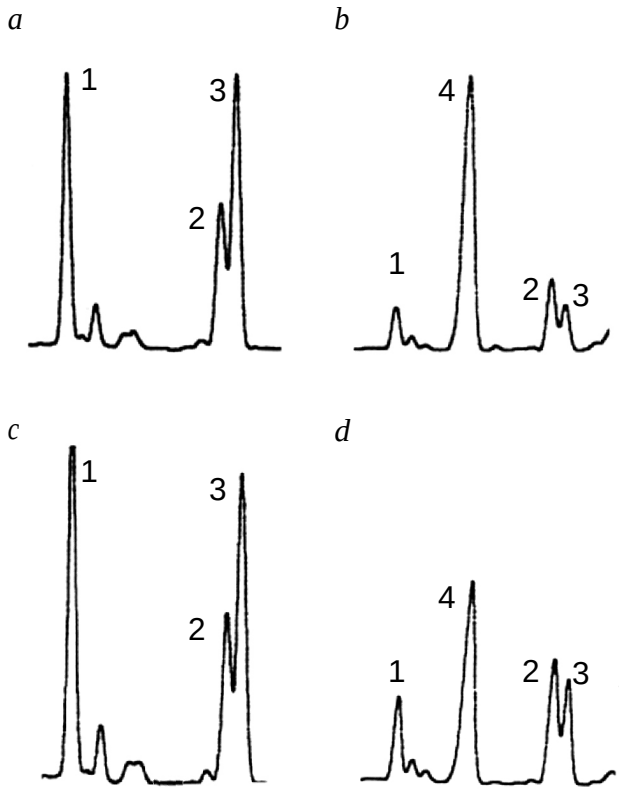

Fig. 3 GC flame ionization profile of sterols extracted from the *erg2-3* strain transformed with vector alone (***a***), wild-type human *EBP* (***b***), human *EBP* containing the E80K mutation (***c***) and human *EBP* containing the R147H mutation (***d***). The results for S133R (data not shown) were the same as those for E80K. The abscissa is elution time and the ordinate, detector response in arbitrary units. The internal standard epicoprostanol is not shown. The major identified compounds are: (1) ergosta-5,8,22-trien-3β-ol; (2) ergosta-8,24(28)-dien-3β-ol (fecosterol); (3) ergost-8-en-3β-ol; (4) ergosta-5,7,22-trien-3β-ol (ergosterol).

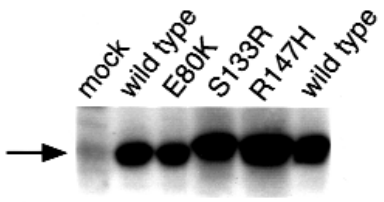

Fig. 4 Sterol-Δ^8-isomerase mutant proteins are stable. Microsomal protein (50 μg) from the *erg2-3* yeast transformed with the indicated N-myc–tagged wild-type or mutant cDNA was separated by SDS–PAGE, blotted and detected with anti-myc antibody. The arrow designates the migration of the 26.4-kD sterol-Δ^8-isomerase[5].

mal only in severe cases (W.R.W., unpublished data). Chondrocytes in reserve cartilage are present singly or in pairs, and surrounded by an avascular matrix. Thus, they may be especially susceptible to metabolic disturbances that are corrected by cross feeding in more densely populated tissues. Recently, the X-linked dominant mouse phenotype tattered (*Td*) was shown to be caused by deficiency of sterol-Δ^8-isomerase[22]. This mouse will provide a useful model to address these pathophysiologic possibilities.

Methods

Sterol analysis of human tissue. The sources of tissue from patients 1–5 have been reported[4]. Fibroblasts from patient 6 were provided by W.R.W.; livers from 7A and 7B were from D. Agamonolis. For analysis of sterol metabolism, we subcultured fibroblasts (1:2) between passages 4–8 in T25 flasks and re-fed them at 24 h and 7 d with RPMI medium containing 15% delipidated fetal calf serum as described[23]. After 14 d growth in delipidated medium, we collected the cells and extracted and quantified the sterols by GC/MS as described[23].

Mutagenesis, transformation and sterol analysis of yeast. We introduced the E80K, S133R and R147H mutations by site-directed mutagenesis into human *EBP* cDNA as described, subcloned them into the 2 μ expression vector YEp351ADC1 (ref. 12) and sequenced them for verification. We transformed the yeast *erg2-3* strain (WAO, his7-2, leu2-3,112 ura3-52 erg2-3; ref. 13) and cultured the transformants in 2% glucose, 0.6% yeast nitrogen base and amino acids minus leucine[5]. For sterol analysis, we cultured yeast in liquid medium for 18 h at 30 °C and then saponified the lipids from 5 mg of cell pellet in 40% KOH (200 μl) in methanol by incubation at 85 °C for 30 min. We extracted, derivitized and separated sterols by GC/MS as described[23]. For detection of sterol-Δ^8-isomerase mutant proteins, we prepared microsomal proteins from the transformed yeast[12]. Our procedures for SDS–PAGE and immunoblotting have been described[24]. We obtained monoclonal antibody to the myc epitope tag from the tissue culture supernatant of the hybridoma 1-9E10 (ATCC).

Mutation analysis. We extracted genomic DNA from fibroblasts, blood and frozen tissue using the Puregene DNA isolation kit (Gentra Systems). We amplified 132–380-bp PCR fragments encompassing isomerase exons and flanking intronic splice sites. Primer pairs for PCR are (sense and antisense): exon 1, 5′–GGGATGTGACAGAGCGCGAG–3′ and 5′–CGCGTAGCCGGGGAGAGC–3′; exon 2, 5′–ATTCGGTCCATTTACATTTCTC–3′ and 5′–CAAATCCCATCCCACAGC–3′; exon 3, 5′–GTGTGTGTTCCTTTCACTGCC–3′ and 5′–GAAAACCAATGCCAGTCTCC–3′; exon 4, 5′–GGTGGTGAGTTGGGGAGCAC–3′ and 5′–CTGGAAGGGCAGCGTTGAGAG–3′; exon 5, 5′–CCTCACTGGGGCTTCTCC–3′ and 5′–CTTCTGGCAGGCAGAGAGC–3′. For PCR we used primer (10 pmol), dNTPs (100 μM), *Taq* polymerase (2.5 U) and 1× standard PCR buffer (Boehringer) in 50 μl. Cycling conditions were 95 °C for 6 min, 35 cycles of 60–65 °C for 10–30 s, 72 °C for 15 s and 95 °C for 30 s, then 72 °C for 10 min. We performed SSCP as described[24] and sequenced electrophoretic variants directly using an automated sequencer. For analysis of the 15G→T polymorphism, we amplified control genomic DNA samples with the exon 2 primer set and the PCR fragment was directly sequenced or digested with *Apa*I (there is loss of a unique *Apa*1 site with 15G→T). We amplified control genomic DNA samples with the exon 2 and exon 4 primer set and performed ASO analysis of the E80K, S133R and R147H allele as described[25]. Control DNA samples were predominantly from the general North American population.

GenBank accession numbers. Human *EBP*, Z37986; *Mus musculus Ebp*, X97755; *Cavia porcellus EBP*, Z37985; *A. thaliana EBP*, AFO30357.

Acknowledgements

We thank the International Skeletal Dysplasia Registry for tissue donations by L. Raffel, A. Soffici, M. Bendon and D. Agamanolis, and G. Nyakatura for providing the DNA sequence of cosmid clone LLNc110A0842 and S. Muscelli for assistance with preparation of this manuscript. This work was supported in part by a NIH grant to the Kennedy Krieger Institute (PO1HD10981, D.V.) and to the General Clinical Research Centers (RR00052 and RR00722, N.B.) and Human Frontiers Sciences Project (F.F.M.), Fonds zur förderung der wissenschaftlichen Forschung (P11636 (HG)) and the Oesterreische Nationalbank (P6515 (HG)). D.V. is an Investigator in the Howard Hughes Medical Institute.

Received 19 March; accepted 25 May 1999.

1. Happle, R. X-linked dominant chondrodysplasia punctata. Review of literature and report of a case. *Hum. Genet.* **53**, 65–73 (1979).
2. Happle, R. X-linked dominant chondrodysplasia punctata/ichthyosis/cataract syndrome in males. *Am. J. Med. Genet.* **57**, 493 (1995).
3. Sutphen, R., Amar, M.J., Kousseff, B.G. & Toomey, K.E. XXY male with X-linked dominant chondrodysplasia punctata (Happle syndrome). *Am. J. Med. Genet.* **57**, 489–492 (1995).
4. Kelley, R.I. *et al.* Abnormal sterol metabolism in patients with Conradi-Hunermann-Happle syndrome and sporadic lethal chondrodysplasia punctata. *Am. J. Med. Genet.* **83**, 213–219 (1999).
5. Hanner, M. *et al.* Phenylalkylamine Ca^{2+} antagonist binding protein. Molecular cloning, tissue distribution, and heterologous expression. *J. Biol. Chem.* **270**, 7551–7557 (1995).
6. Schindelhauer, D. *et al.* Long-range map of a 3.5-Mb region in Xp11.23–22 with a sequence-ready map from a 1.1-Mb gene-rich interval. *Genome Res.* **6**, 1056–1069 (1996).
7. Tint, G.S. *et al.* Defective cholesterol biosynthesis associated with the Smith-Lemli-Opitz syndrome. *N. Engl. J. Med.* **330**, 107–113 (1994).
8. Fitzky, B.U. *et al.* Mutations in the Δ^7-sterol reductase gene in patients with the Smith-Lemli-Opitz syndrome. *Proc. Natl Acad. Sci USA* **95**, 8181–8186 (1998).
9. Bjorkhem, I. *et al.* Correlation between serum levels of cholesterol precursors and activity of HMG-CoA reductase in human liver. *J. Lipid Res.* **28**, 1137–1143 (1987).
10. Moebius, F.F. *et al.* Purification and amino-terminal sequencing of the high affinity phenylalkylamine Ca^{2+} antagonist binding protein from guinea pig liver endoplasmic reticulum. *J. Biol. Chem.* **269**, 29314–29320 (1994).
11. Silve, S. *et al.* Emopamil-binding protein, a mammalian protein that binds a series of structurally diverse neuroprotective agents, exhibits Δ^8-Δ^7 sterol isomerase activity in yeast. *J. Biol. Chem.* **271**, 22434–22440 (1996).
12. Moebius, F.F. *et al.* Histidine77, glutamic acid81, glutamic acid123, threonine126, asparagine194, and tryptophan197 of the human emopamil binding protein are required for *in vivo* sterol Δ^8-Δ^7 isomerization. *Biochemistry* **38**, 1119–1127 (1999).
13. Ashman, W.H., Barbuch, R.J., Ulbright, C.E., Jarrett, H.W. & Bard, M. Cloning and disruption of the yeast C-8 sterol isomerase gene. *Lipids* **26**, 628–632 (1991).
14. Herman, G.E. & Walton, S.J. Close linkage of the murine locus bare patches to the X-linked visual pigment gene: implications for mapping human X-linked dominant chondrodysplasia punctata. *Genomics* **7**, 307–312 (1990).
15. Herman, G.E. *et al.* The gene mutated in bare patches and striated mice encodes a novel 3β-hydroxysteroid dehydrodenase. *Nature Genet.* **22**, 182–187 (1999).
16. FitzPatrick, D.R. *et al.* Clinical phenotype of desmosterolosis. *Am. J. Med. Genet.* **75**, 145–152 (1998).
17. Cooper, M.K., Porter, J.A., Young, K.E. & Beachy, P.A. Teratogen-mediated inhibition of target tissue response to Shh signaling. *Science* **280**, 1603–1607 (1998).
18. Porter, J.A., Young, K.E. & Beachy, P.A. Cholesterol modification of hedgehog signaling proteins in animal development. *Science* **274**, 255–259 (1996).
19. Karaplis, A.C. *et al.* Lethal skeletal dysplasia from targeted disruption of the parathyroid hormone-related peptide gene. *Genes Dev.* **8**, 277–289 (1994).
20. Lanske, B. *et al.* PTH/PTHrP receptor in early development and Indian hedgehog-regulated bone growth. *Science* **273**, 663–666 (1996).
21. Chuang, P.T. & McMahon, A.P. Vertebrate Hedgehog signalling modulated by induction of a Hedgehog-binding protein. *Nature* **397**, 617–621 (1999).
22. Derry, J.M.J *et al.* Mutations in a Δ^8-Δ^7 sterol isomerase in the tattered mouse and X-linked dominant chondrodysplasia punctata *Nature Genet.* **22**, 286-293 (1999).
23. Kelley, R.I. Diagnosis of Smith-Lemli-Opitz syndrome by gas chromatography/mass spectrometry of 7-dehydrocholesterol in plasma, amniotic fluid and cultured skin fibroblasts. *Clin. Chim. Acta* **236**, 45–58 (1995).
24. Brody, L.C. *et al.* Ornithine-δ-aminotransferase mutations causing gyrate atrophy: allelic heterogeneity and functional consequences. *J. Biol. Chem.* **267**, 3302–3307 (1992).
25. Braverman, N. *et al.* Human *PEX7* encodes the peroxisomal PTS2 receptor and is responsible for rhizomelic chondrodysplasia punctata. *Nature Genet.* **15**, 369–376 (1997).